

# Formation of cyanide-functionalized SBA-15 and its transformation to carboxylate-functionalized SBA-15

Chia-min Yang, Yanqin Wang, Bodo Zibrowius and Ferdi Schüth\*

Max-Planck-Institut für Kohlenforschung, Kaiser-Wilhelm-Platz 1, D 45470 Mülheim an der Ruhr, Germany. E-mail: [schueth@mpi-muelheim.mpg.de](mailto:schueth@mpi-muelheim.mpg.de); Tel: +49 208 306 2373

Received 12th November 2003, Accepted 24th February 2004  
First published as an Advance Article on the web 18th March 2004

Cyanide-functionalized mesoporous silica SBA-15 (CN/SBA-15) with pore diameters larger than 6 nm has been prepared by a one-pot synthesis. The structure of CN/SBA-15 is affected by the amount of the functional silane 2-cyanoethyltriethoxysilane (CTES) and the conditions of co-condensation in the acidic aqueous solution of the triblock copolymer Pluronic P123: whereas direct mixing of the silica sources CTES and tetraethoxysilane (TEOS) leads to a disordered hybrid material, a highly ordered CN/SBA-15 is obtained if the synthesis solution containing CTES is prepared first and TEOS added afterwards. Treatment of the as-synthesized materials with concentrated sulfuric acid removes the copolymer template through ether cleavage and hydrolyses the –CN groups in one step, resulting in carboxylate-functionalized SBA-15 (CA/SBA-15).  $^{13}\text{C}$  CP/MAS NMR spectra show that for some CN/SBA-15 materials the copolymer template can be totally removed in this way, suggesting that all the hydrophilic ethylene oxide (EO) chains of the template are accessible to the acid. Nitrogen sorption measurements also indicate that these materials contain nearly no micropores in contrast to the pure-silica SBA-15 synthesized under the same conditions, which has a considerable proportion of micropores. The results suggest that the structural order and microstructures of the resulting CN/SBA-15 materials are strongly affected by assembly kinetics, which involve the hydrolysis and condensation of silica species and their interaction with the template.

## 1. Introduction

The advent of ordered mesoporous materials has sparked worldwide scientific interest. Following the discovery of MCM-41-type mesoporous materials templated by cationic surfactant micelles,<sup>1,2</sup> various preparation methods for ordered mesoporous materials have been introduced.<sup>3–6</sup> In 1998, a new synthesis route for ordered mesoporous silicas was reported that uses poly(alkylene oxide) triblock copolymers as templates in an acidic medium.<sup>7,8</sup> SBA-15, with its hexagonally arranged one-dimensional pores, is a member of this family of mesoporous silicas. These new materials have large surface areas and larger pore sizes and better thermal and hydrothermal stabilities than MCM-41-type materials. Their discovery initiated intensive research on their synthesis and potential applications.

One of the most promising applications of ordered mesoporous materials is to serve as scaffolds for constructing functional composite materials with defined spatial arrangements on the nanometer scale.<sup>9,10</sup> Guest molecules or clusters can be incorporated either in the mesopores or into the pore walls.<sup>11–14</sup> On the other hand, organic functional groups can also be introduced into the silica walls, forming an organic–inorganic hybrid,<sup>15–20</sup> or can be tethered to the pore surface through surface modification.<sup>20–22</sup> The surface modification can be achieved by post-synthesis treatments such as grafting and coating reactions.<sup>20</sup> Alternatively, the pore surface can also be functionalized by direct co-condensation (or called “one-pot” synthesis) of the functional silanes with tetraalkoxysilanes as the primary silica source.<sup>20</sup> The one-pot synthesis has the advantage of allowing better control of the concentration of functional groups in the product. In addition, it avoids tedious procedures for the post-synthesis functionalization such as rehydroxylation to achieve higher density of silanol

groups on the pore surface, and washing and filtration after functionalization. However, such a synthetic route can only be used when no significant phase separation occurs and if the Si–C bond of the functional silane is preserved during the synthesis and removal of the template. Many functional silanes with functionalities such as mercaptopropyl, aminopropyl, phenyl, vinyl or other alkyl groups have been incorporated into mesoporous silicas through the one-pot synthesis route.<sup>20,21</sup>

Recently, we have focused on one-pot syntheses of modified mesoporous silicas with functional groups that are reactive enough for further modification.<sup>22–24</sup> One of the target materials is cyanide (–CN) functionalized mesoporous silica SBA-15. The cyanide groups can complex with some metal ions, or can either be selectively reduced to an aldehyde or reacted with Grignard reagents to form ketones. They can also be hydrolysed to carboxylate (–COOH) groups, which can serve as anchor sites for biomolecules and for protein synthesis in SBA-15.<sup>25</sup> In addition, the –COOH groups are moderately acidic and they de-protonate and become negatively charged under neutral and basic conditions. The electrostatic interaction between –COOH groups and transition metal ions opens up the possibility of preparing SBA-15-supported nanostructured metal or metal oxide catalysts.

We have already demonstrated the synthesis of –CN-functionalized SBA-15 (CN/SBA-15) and its transformation to –COOH-functionalized SBA-15 (CA/SBA-15) by treatment with sulfuric acid.<sup>22</sup> This can remove the triblock copolymer template and hydrolyse the –CN groups in one step without shrinkage of the silica matrix. In the present paper, we report in more detail on the formation of CN/SBA-15 materials by one-pot synthesis and the removal of the template and transformation to CA/SBA-15. Special attention is devoted to physicochemical characterization of the materials at these different stages of preparation.

Our results suggest that the structure of the materials is strongly dependent upon the assembly kinetics of the silica hydrolysis/condensation and the interaction between the functional silica species and the triblock copolymer template. Usually, functionalized ordered mesoporous materials are synthesized by simply mixing the silica sources and hydrolysing them together.<sup>20</sup> To prepare the materials reported here, it was necessary to hydrolyse the functional silane in the template-containing acidic solution for a certain period of time before the tetraalkoxysilane was added.

## 2. Experimental

### Materials

CN/SBA-15 materials were synthesized at 40 °C by using the triblock copolymer Pluronic P123 ((EO)<sub>20</sub>(PO)<sub>70</sub>(EO)<sub>20</sub>, BASF) as template. 2-Cyanoethyltriethoxysilane (CTES, Gel-est) was added to the hydrochloric acid solution of Pluronic P123 and stirred for up to 1 h. Tetraethoxysilane (TEOS) was then added to the mixture. Further syntheses were carried out with a pre-mixed solution of CTES and TEOS. The molar composition of the mixture was (1 - *x*) TEOS:*x* CTES:*y* HCl:193 H<sub>2</sub>O:0.017 P123, where *x* = 0.1 to 0.5, and *y* = 4.0 to 7.0. The mixture was stirred for 20 h, followed by aging at 60 °C or 90 °C without stirring for 24 h. The products were filtered without washing and then dried at 80 °C.

The CN/SBA-15 materials were treated with 48 wt.% H<sub>2</sub>SO<sub>4</sub> solution at 95 °C to cleave the template and produce CA/SBA-15. A typical treatment involved stirring 1.0 g CN/SBA-15 material in 150 mL H<sub>2</sub>SO<sub>4</sub> solution for 24 h. The treated solids were washed with water until the eluent became neutral and then dried at 60 °C. Throughout this paper, the materials are referred to as *xx-yy-zz/CN* (CN/SBA-15) or *xx-yy-zz/CA* (CA/SBA-15), where *xx* denotes the aging temperature in °C, *yy* is the time in minutes the synthesis mixture was stirred before TEOS was added (for the pre-mixed silica source, *yy* = P), and *zz* is the molar percentage of CTES (e.g., 10 for 10%). For example, 60-30-10/CN refers to a CN/SBA-15 sample aged at 60 °C with 10% CTES in the synthesis mixture and a delay time of 30 min for the addition of TEOS. The pure-silica SBA-15 materials are referred to as *xx-AS* (as-synthesized SBA-15) or *xx-AT* (acid-treated SBA-15), where *xx* denotes the aging temperature in °C.

### Characterization

Powder X-ray diffraction data (PXRD) were obtained on a Stoe STADI P diffractometer in the reflection mode using Cu K $\alpha$  radiation. Nitrogen sorption isotherms were measured at 77 K using a Micromeritics ASAP 2010 instrument. Each sample was evacuated at 80 °C for 12 h. The BET surface area was calculated from the adsorption branches in the relative pressure range of 0.05–0.20, and the total pore volume was evaluated at a relative pressure of 0.98. The pore diameter and the pore size distribution were calculated from the desorption branch using the Barrett–Joyner–Halenda (BJH) method. For *t*-plot analyses, the Harkins–Jura equation with standard parameters obtained from nonporous reference material was used. The solid-state NMR spectra were measured on a Bruker Avance 500WB spectrometer using a 4-mm MAS probe at a spinning rate of 10 kHz. The experimental conditions for <sup>13</sup>C CP/MAS NMR were 2 s recycle delay, 20 000 scans, 1 ms contact time, and 4.4  $\mu$ s <sup>1</sup>H  $\pi/2$  pulse and those for <sup>29</sup>Si MAS NMR were 30 s recycle delay, 2400 scans, and 2.2  $\mu$ s  $\pi/4$  pulse. The weight loss curves of the functionalized SBA-15 materials under an air atmosphere were measured on a TG/DTA instrument (Netzsch STA 449 C) with a heating rate of 5 K min<sup>-1</sup>.

## 3. Results and discussion

Although CN/SBA-15 materials can be prepared in the whole concentration range given above, the optimum ratio of TEOS to HCl to produce the highly ordered hexagonal structure was found to be 1:5:8. This ratio was applied for the samples discussed in the following. The maximum molar percentage of CTES as the silica source for ordered materials aged at 90 °C was found to be around 40%, while for samples aged at 60 °C the maximum percentage was found to be around 30%. When a larger amount of CTES was added to the synthesis mixture, only disordered materials were obtained. We focus on the structural studies of materials prepared with 10% and 20% CTES.

The structural ordering and the pore diameters are very sensitive to the way CTES and TEOS are mixed. For example, Fig. 1a shows the PXRD patterns of the materials with 10% CTES aged at 90 °C. If CTES is pre-mixed with TEOS as the silica source (sample 90-P-10/CN), the resulting material is amorphous. However, when TEOS is added to the synthesis mixture after CTES, the products show three reflections attributed to a hexagonal structure. The structural order increases and the cell dimensions become slightly larger on lengthening the period over which the mixture is stirred before TEOS is added. The cell dimensions seem to approach a maximum value of 11.5 nm when this period is greater than 30 min, since the positions of the reflections are the same for samples 90-30-10/CN and 90-60-10/CN. However, the reflections for 90-60-10/CN are more intense than those for 90-30-10/CN, suggesting that structural order has improved.

The samples were treated with 48 wt.% H<sub>2</sub>SO<sub>4</sub> at 95 °C to decompose the copolymer template and vacate the mesopores. As Fig. 1b shows, the (110) and (200) reflections of the treated samples are better resolved and more intense than

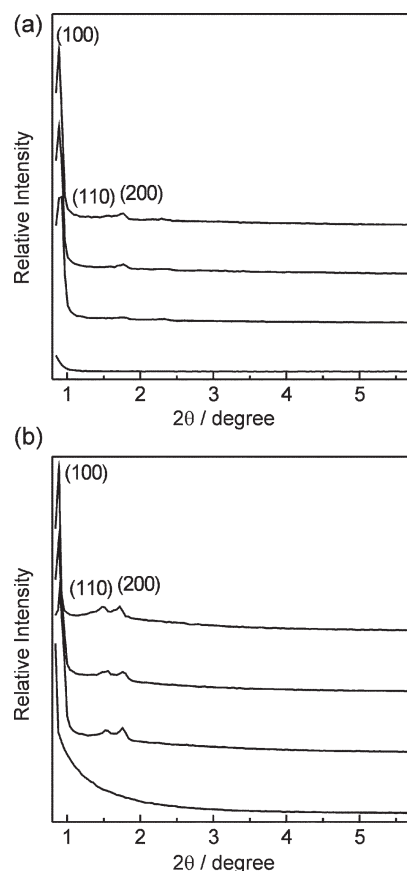


**Fig. 1** PXRD patterns of the samples 90-P-10/CN, 90-00-10/CN, 90-30-10/CN and 90-60-10/CN (from bottom to top) before (a) and after (b) treatment with H<sub>2</sub>SO<sub>4</sub>.

those of the as-prepared sample, because of the increased X-ray scattering contrast between the silica wall and the pore. For all the samples (except 90-P-10/CA, with no reflection), the positions of the reflections were unchanged after the template had been removed, indicating that there is no shrinkage of the cell dimensions of the materials. The nitrogen sorption isotherms of these materials are shown in Fig. 2a. Except for 90-P-10/CA, the sorption isotherms show sharp steps with hysteresis loops corresponding to the filling of ordered mesopores. The pore size distributions calculated from the desorption branches using the BJH method are shown in Fig. 2b. The sample 90-P-10/CA exhibits a low pore volume and a wide pore size distribution, while all the other materials show narrow distributions. In addition, the average BJH pore diameter increases when the synthesis mixture is stirred for longer before TEOS is added, and it approaches a maximum size of 7.4 nm. A similar influence of this delay time on cell dimension, pore structure and pore diameter has also been observed for other series of materials with 10% or 20% CTES aged at either 90 °C or 60 °C.

The results of the physicochemical characterization, summarized in Table 1, allow conclusions on the formation mechanism to be drawn. It is known that during the synthesis of SBA-15 the ethylene oxide (EO) chains become less hydrophilic at higher temperature due to the partial dehydration.<sup>26</sup> Such an effect weakens the interaction between the EO chains and the silica, so that the size of the copolymer micelles (corresponding to the mesopore diameter after template removal) increases when the materials are aged at higher temperature. The same temperature dependence was found for the CN/SBA-15 materials regardless of the amount of CTES in the

synthesis mixture. However, the cell dimensions and the pore diameters of the CA/SBA-15 materials are slightly smaller than those of pure-silica SBA-15 aged at the same temperature and treated with sulfuric acid under the same conditions. In addition, TG/DTA analyses of the CN/SBA-15 materials show two exothermic decomposition steps at about 210 °C and 365 °C, attributed to the Pluronic P123 template and the cyanoethyl groups, respectively. The decomposition temperature of P123 in CN/SBA-15 is slightly higher than that in the pure-silica SBA-15 (about 160 °C). Generally, the CN/SBA-15 materials exhibit a weight loss of around 35% which is attributed to the decomposition of P123 in the temperature range of 150 °C to 300 °C. Hence, the amount of P123 is significantly lower than in the as-prepared pure-silica SBA-15 (about 50 wt.%).<sup>27,28</sup> The smaller pore diameters and the lower amounts of P123 in the as-prepared CN/SBA-15 materials suggest a smaller aggregation number (*i.e.* the number of monomers in the micelle) of P123 in the formation of CN/SBA-15 compared to that for pure-silica SBA-15.

The CN/SBA-15 materials aged at 90 °C (90-60-10/CN and 90-60-20/CN) are highly ordered, while the structure of the materials aged at 60 °C was found to be affected by the amount of CTES added to the synthesis mixture. Fig. 3 shows the PXRD patterns of samples aged at 60 °C. The better-defined reflections for 60-AS and 60-60-10/CN indicate a better structural ordering compared with 60-60-20/CN. After removal of the template, the (110) and (200) reflections of the PXRD patterns become better resolved but do not shift. Hence, the cell dimension is not changed during the treatment. It should be noted that the cell dimension of 60-60-20/CA is slightly smaller than that of 60-AT. The nitrogen sorption measurements of the three materials (Fig. 4) show that the hysteresis shifts slightly to lower relative pressure and the steps become less steep as the percentage of CTES in the synthesis mixture is increased, indicating a smaller pore diameter and a wider pore size distribution.

The necessity for a delay period before TEOS is added if ordered CN/SBA-15 materials are to be formed contrasts with other co-condensation preparations of functional mesoporous silicas.<sup>20</sup> Furthermore, in comparison with pure-silica SBA-15 synthesized under the same conditions, the amounts of P123 in CN/SBA-15 and the pore diameters in CA/SBA-15 are smaller. These results suggest that the hydrolysis and condensation of CTES prior to the addition of TEOS and the possible interaction between CTES or pre-formed silica species and the P123 micelles affect the whole assembly process. The cyanoethyl moiety of CTES is hydrophobic with a polar –CN head group. The cyanoethyl groups do not seem to be hydrophobic enough to act as a cosurfactant as in other systems with aliphatic alcohols or hydrophobic functional silanes.<sup>24,29,30</sup> A cosurfactant would be adsorbed close to the hydrophobic core of poly(propylene oxide) (PPO) in the P123 micelles, decreasing the interfacial curvature and leading to a transformation of the overall structure. However, in the ranges of synthesis conditions applied, we never observed such a phenomenon and always obtained hexagonal materials. The hydrolysis of the ethoxy groups of CTES is fast under the acidic synthesis conditions and might even be faster than for TEOS because of the electron-donating effect of the cyanoethyl group.<sup>31</sup> On the other hand, the hydrophobicity of the functional silane is changed substantially by hydrolysis of the –CN group of CTES. This reaction might occur at the higher temperature during the aging process, but it is not likely to take place during assembly at the relatively low temperature of 40 °C (see below). The hydrolysed CTES might pre-form a partially condensed silica species and interact with the P123 micelles, and lead to a reduced aggregation number of P123 during the subsequent assembly process. The polar –CN groups might also play a role in the formation of ordered CN/SBA-15 materials. The formation mechanism of CN/SBA-15 materials, however,

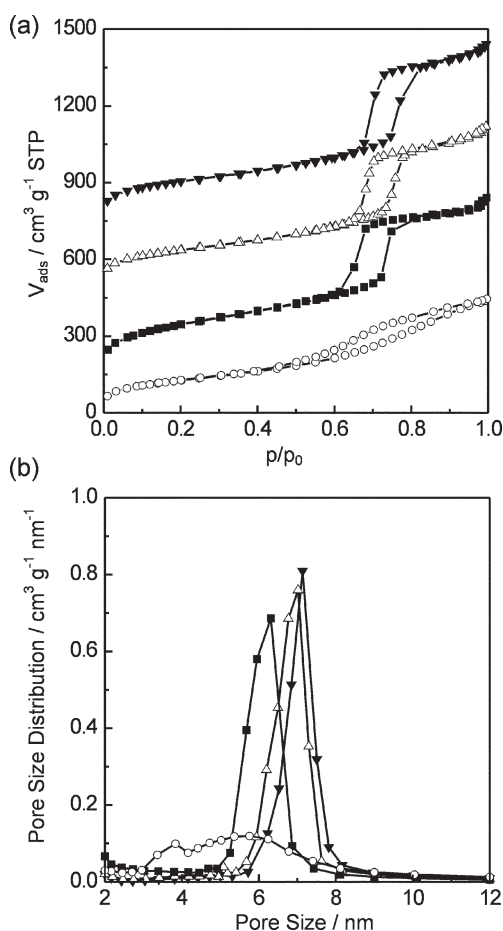


**Fig. 2** Nitrogen sorption isotherms (a) and pore size distributions (b) of the samples 90-P-10/CA (○), 90-00-10/CA (■), 90-30-10/CA (△) and 90-60-10/CA (▼). The isotherms in (a) are shifted by 0, 250, 500 and 750 cm<sup>3</sup> g<sup>-1</sup> STP, respectively.

**Table 1** Comparison of physicochemical properties of –COOH-functionalized and pure-silica SBA-15 materials<sup>a</sup>

Sample	Cell dimension/nm	Pore diameter/nm	BET surface area/m <sup>2</sup> g <sup>-1</sup>	Total pore volume/cm <sup>3</sup> g <sup>-1</sup>	Micropore volume <sup>b</sup> /cm <sup>3</sup> g <sup>-1</sup>
60-AT	10.9	6.8	476	0.77	0.13
60-00-10/CA	10.2	6.2	459	0.64	0.02
60-60-10/CA	10.6	6.5	470	0.68	0.02
60-60-10/CA <sup>c</sup>	10.6	6.5	471	0.68	0.06
60-00-20/CA	10.1	6.2	438	0.59	0.02
60-60-20/CA	10.3	6.3	463	0.63	0.02
60-60-20/CA <sup>c</sup>	10.3	6.3	461	0.63	0.02
90-AT	11.8	7.7	638	1.11	0.08
90-00-10/CA	11.2	7.2	565	1.01	0.01
90-60-10/CA	11.5	7.4	589	1.01	0.01
90-00-20/CA	11.0	7.1	521	0.90	0.01
90-60-20/CA	11.3	7.2	533	0.92	<0.01

<sup>a</sup> The pore walls of all the samples are (4.0 ± 0.1) nm thick (except 60-AT, 4.2 nm). <sup>b</sup> From *t*-plots. <sup>c</sup> The samples were heated to 250 °C for 3 h.

cannot be fully elucidated based on the observations discussed above, and further kinetic studies are necessary.

The removal of the template P123 by treatment with sulfuric acid and its effect on the silica matrix were monitored by solid-state NMR spectroscopy. Fig. 5 shows <sup>13</sup>C CP/MAS NMR spectra of samples aged at 90 °C. The spectra of the materials before the acid treatment contain lines that can be attributed to the copolymer template Pluronic P123 (76.0 ppm, 73.7 ppm, 70.7 ppm and 16.6 ppm) and the cyanoethyl groups (122 ppm and 10 ppm). The resolution obtained for the lines of the template is significantly better than previously observed for materials washed with solvent,<sup>22</sup> suggesting that residual

bulk copolymer might adhere on the outer surface of the hybrid materials. The small lines at 178 ppm and 27 ppm indicate that some of the –CN groups are hydrolysed to –COOH groups before the acid treatment. On the other hand, the <sup>13</sup>C NMR spectra of materials aged at 60 °C (Fig. 6) show no hydrolysed –CN groups prior to acid treatment. Apparently, the partial hydrolysis of –CN groups in the samples aged at 90 °C is caused by the higher aging temperature in the acidic aqueous solution.

The <sup>13</sup>C NMR spectra of the acid-treated samples are dominated by the resonance lines of the –(CH<sub>2</sub>)<sub>2</sub>–COOH groups (178 ppm, 27.4 ppm and 7.6 ppm). Obviously, these three lines do not have equal intensities. Since the efficiency of the cross-polarization strongly decreases with increasing distance between the <sup>13</sup>C and the <sup>1</sup>H nuclei, the intensities of both the –CN and the –COOH lines are reduced compared to those of the methylene lines. However, our results show that <sup>13</sup>C CP/MAS NMR spectroscopy can be used to follow the fate of functional groups during the removal of the template from functionalized mesoporous materials. The changes observed for the line of one of the methylene groups corroborates the conclusions drawn. No line indicating the presence of –CN groups was found for any of the materials treated with 48 wt.% H<sub>2</sub>SO<sub>4</sub>. Hence, the hydrolysis of –CN groups by H<sub>2</sub>SO<sub>4</sub> at 95 °C is very efficient and all –CN groups are accessible to the acid. Furthermore, the <sup>13</sup>C NMR spectra of 90-60-20/CA and 60-60-20/CA show a complete removal of the

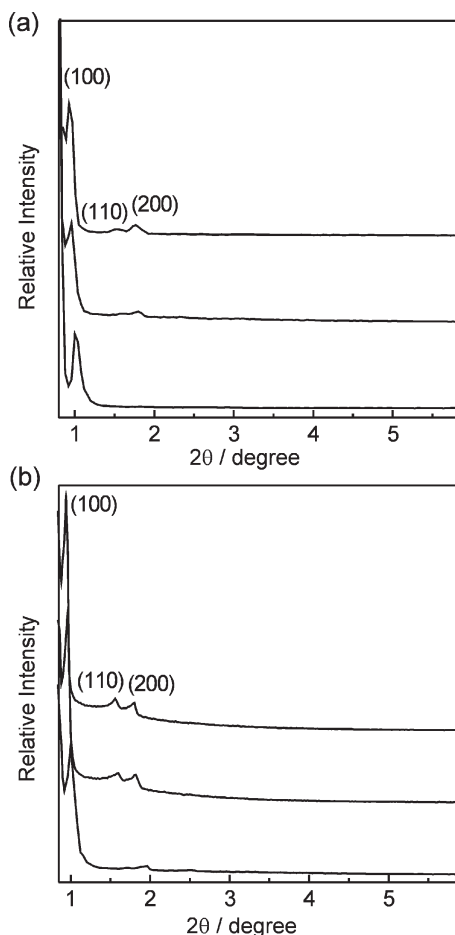


**Fig. 3** PXRD patterns of the samples 60-AS, 60-60-10/CN, 60-60-20/CN (from top to bottom) before (a) and after (b) treatment with H<sub>2</sub>SO<sub>4</sub>.

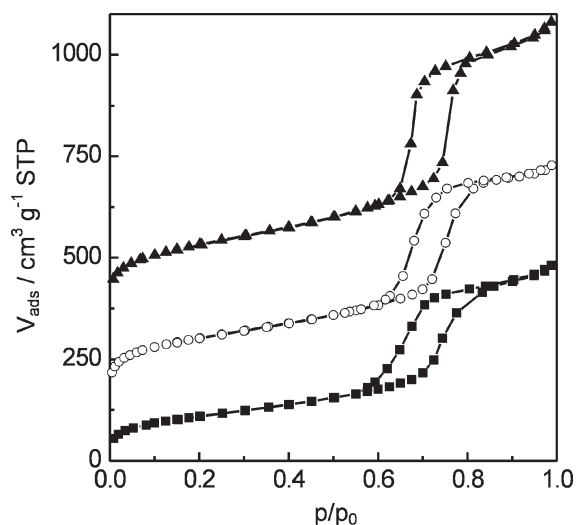


**Fig. 4** Nitrogen sorption isotherms of the samples 60-60-20/CA (■), 60-60-10/CA (○) and 60-AT (▲). The isotherms are shifted by 0, 200 and 400 cm<sup>3</sup> g<sup>-1</sup> STP, respectively.

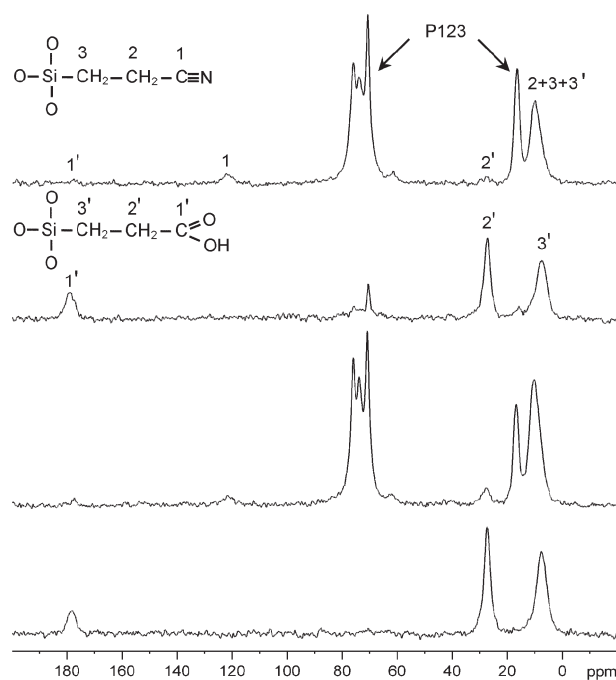


Fig. 5  $^{13}\text{C}$  CP/MAS NMR spectra of the samples 90-60-10/CN, 90-60-10/CA, 90-60-20/CN and 90-60-20/CA (from top to bottom).

copolymer template in CN/SBA-15 samples through ether cleavage. The spectra of 90-60-10/CA and 60-60-10/CA, however, contain small lines stemming from residual EO chains. It has been shown that for the as-prepared pure-silica SBA-15, the EO chains left in the material after the same acid treatment are occluded in the silica matrix and are not accessible to the acid.<sup>32</sup> Therefore, the results suggest that, in the samples synthesized with 20% CTES, the EO chains are not incorporated in the silica matrix during the synthesis regardless of the aging temperature. This is again very different from the pure-silica SBA-15, where micropores resulting from the removal of occluded EO-moieties can contribute to up to 30% of the total pore volume.<sup>26</sup>

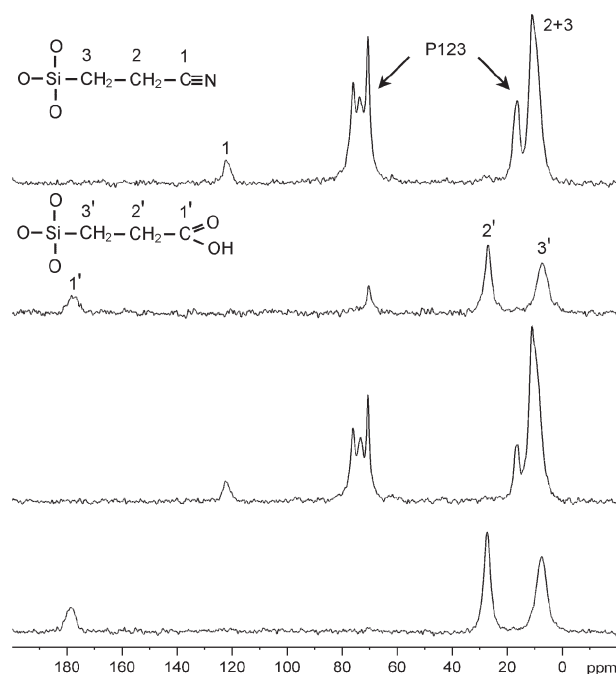


Fig. 6  $^{13}\text{C}$  CP/MAS NMR spectra of the samples 60-60-10/CN, 60-60-10/CA, 60-60-20/CN and 60-60-20/CA (from top to bottom).

Fig. 7 shows  $^{29}\text{Si}$  MAS NMR spectra of materials aged at  $60^\circ\text{C}$  containing different amounts of functional groups. These spectra exhibit basically two kinds of lines, namely lines attributed to  $T^n$  groups ( $\text{Si}(\text{OSi})_n(\text{OH})_{3-n}\text{C}$ ) stemming from the silicon of the functional silane and lines attributed to  $Q^n$  groups ( $\text{Si}(\text{OSi})_n(\text{OH})_{4-n}$ ) of the silica backbone. The integral intensities of the lines of the T groups correspond to the fraction of silicon atoms bearing a functional group. Although a better signal-to-noise ratio would be desirable, the quality of the spectra is sufficient to obtain reliable estimates ( $\pm 3\%$ ) of the proportions of T groups. The data for the individual lines given in Table 2 are adjusted to the ratios of the integrals of the T and Q regions.

The fractions of T groups present in some of the materials are somewhat smaller than could be expected from the molar ratios of silicon compounds used in the starting synthesis mixtures. However, the overall intensities of the lines assigned to T groups are little affected by the acid treatment, indicating that the functional groups are strongly anchored to the silica. For the Q groups, the relative intensities of the  $Q^2$  and  $Q^3$  lines are reduced after the acid treatment, while the  $Q^4$  line becomes more intense. This observation suggests that during the treatment at  $95^\circ\text{C}$ , the acid does not just cleave the template and hydrolyse the  $-\text{CN}$  groups, but also facilitates a further condensation of silanol groups in the pore walls, as has been described previously.<sup>22,32</sup>

The microporosity of the materials was checked by  $t$ -plot analysis, and the data are included in Table 1. For all the CA/SBA-15 samples, only mesopores and nearly no micropores were found after acid treatment. This result is consistent with that obtained for the pure-silica SBA-15, since only the copolymer chains that are accessible to the acid can be cleaved and removed.<sup>32</sup> To completely remove the EO chains, three samples, *i.e.* 60-AT, 60-60-10/CA and 60-60-20/CA, were calcined at  $250^\circ\text{C}$  for 3 h in air. A calcination temperature higher than  $250^\circ\text{C}$  was not used in order to avoid shrinkage during high-temperature treatment and to retain the microstructure of the silica matrix. TG/DTA measurement shows that the surface functional groups (*i.e.*  $-(\text{CH}_2)_2-\text{COOH}$  groups) decompose at around  $285^\circ\text{C}$  and  $400^\circ\text{C}$ . Fig. 8 shows the  $t$ -plots of the three materials after calcination at  $250^\circ\text{C}$ . In the micropore region, the  $t$ -plot for 60-AT gives a straight line between  $t = 0.45$  and  $t = 0.75$  nm, whereas the  $t$ -plots for

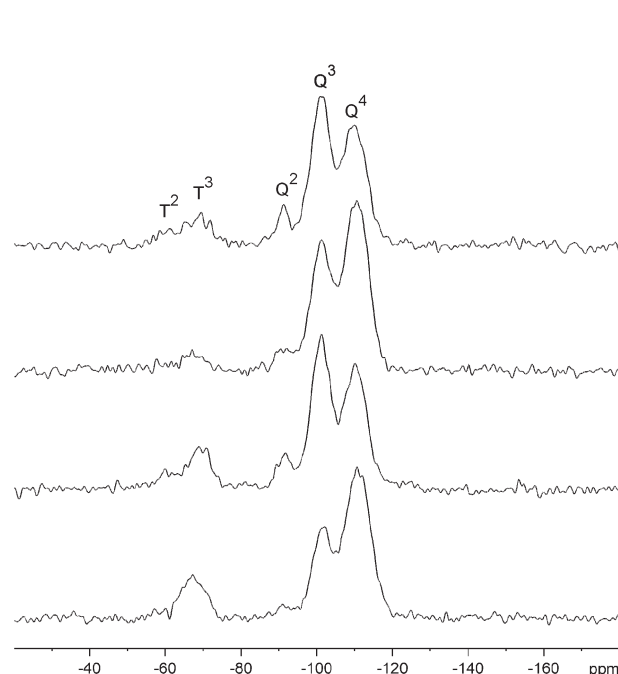


Fig. 7  $^{29}\text{Si}$  MAS NMR spectra of the samples 60-60-10/CN, 60-60-10/CA, 60-60-20/CN and 60-60-20/CA (from top to bottom).

**Table 2** Relative intensities of the  $^{29}\text{Si}$  NMR lines assigned in Fig. 7

Sample	T <sup>2</sup>	T <sup>3</sup>	Q <sup>2</sup>	Q <sup>3</sup>	Q <sup>4</sup>
60-60-10/CN	3	7	8	40	41
60-60-10/CA	1	6	5	35	53
60-60-20/CN	4	12	7	40	37
60-60-20/CA	2	15	3	27	53

60-60-10/CA and 60-60-20/CA give straight lines between  $t = 0.40$  and  $t = 0.80$  nm. The  $y$ -intercept for 60-AT is about twice that for 60-60-10/CA, which is itself twice that for 60-60-20/CA, indicating that the micropore volume of the three materials are different. Hence, the micropore volume is related to the amount of EO units left in the materials after treatment with  $\text{H}_2\text{SO}_4$ , which is in turn affected by the molar ratio of CTES present in the synthesis mixture.

It should be mentioned that the surface properties of CA/SBA-15 materials are distinct from that of the nonporous reference silica sample. To estimate the effect of surface functionality on the  $t$ -plot analysis, a  $-\text{COOH}$ -functionalized aerosil (Aerosil 200, Degussa) was prepared by reacting the aerosil with CTES and then hydrolysing the product with sulfuric acid. The  $t$ -plots of the parent and functionalized aerosils based on the nonporous silica reference were compared. The derived microporosity of functionalized aerosil was 11% larger than that for the parent aerosil, suggesting that the microporosity of the CA/SBA-15 might be slightly overestimated.

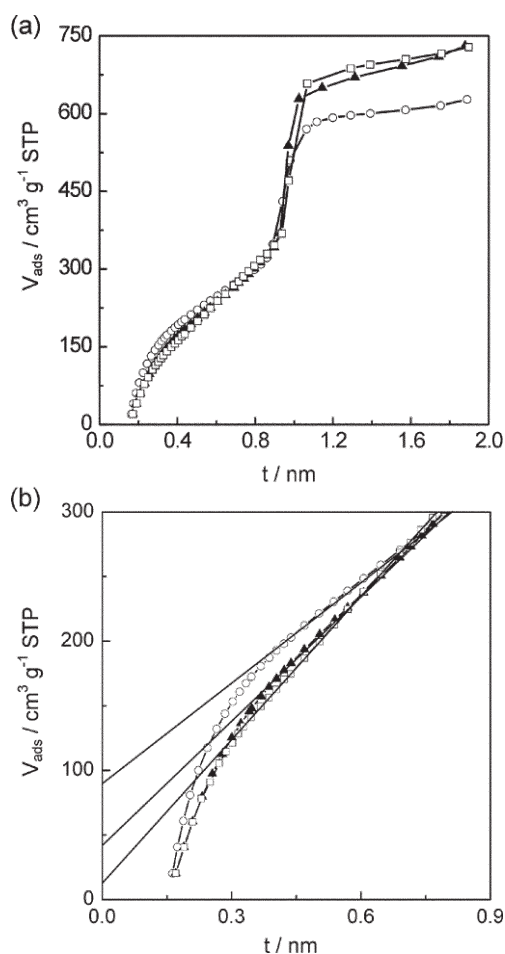


**Fig. 8** (a) Nitrogen  $t$ -plots of the samples 60-AT (○), 60-60-10/CA (▲) and 60-60-20/CA (□) after calcination at 250 °C. (b) Magnification of the low  $t$ -value part ( $t = 0$  nm to 0.9 nm) of the curves in (a).

## 4. Conclusion

CN/SBA-15 materials have been prepared by the co-condensation of CTES and TEOS. It has been found that, to form the hexagonally ordered structure, a delay period is required before TEOS is added to the synthesis mixture. The percentage of CTES in the synthesis mixture, the delay time and the aging temperature affect the structure of the resulting materials. Removal of the copolymer template and the hydrolysis of  $-\text{CN}$  groups to  $-\text{COOH}$  groups can be achieved in one step by treatment with sulfuric acid. The results suggest that formation of ordered CN/SBA-15 materials relies on the right assembly kinetics involving the hydrolysis and condensation of silica species and the interaction between the P123 micelles and these silica species. The fraction of micropores in the walls of the cyanide- and carboxylate-functionalized materials is strongly reduced compared to regular SBA-15.

## Acknowledgements

The authors thank Drs W. Schmidt, M. Lindén, F. Kleitz and R. Mynott for fruitful discussions.

## References

- C. T. Kresge, M. E. Leonowicz, W. J. Roth, J. C. Vartuli and J. S. Beck, *Nature*, 1992, **359**, 710.
- J. S. Beck, J. C. Vartuli, W. J. Roth, M. E. Leonowicz, C. T. Kresge, K. D. Schmitt, C. T.-W. Chu, D. H. Olson, E. W. Sheppard, S. B. McCullen, J. B. Higgins and J. L. Schlenker, *J. Am. Chem. Soc.*, 1992, **114**, 10834.
- J. Y. Ying, C. P. Mehnert and M. S. Wong, *Angew. Chem. Int. Ed.*, 1999, **38**, 56.
- U. Ciesla and F. Schüth, *Microporous Mesoporous Mater.*, 1999, **27**, 131.
- A. Sayari and S. Hamoudi, *Chem. Mater.*, 2001, **13**, 3151.
- G. J. de, A. A. Soler-Illia, C. Sanchez, B. Lebeau and J. Patarin, *Chem. Rev.*, 2002, **102**, 4093.
- D. Zhao, J. Feng, Q. Huo, N. Melosh, G. H. Fredrickson, B. F. Chmelka and G. D. Stucky, *Science*, 1998, **279**, 548.
- D. Zhao, Q. Huo, J. Feng, B. F. Chmelka and G. D. Stucky, *J. Am. Chem. Soc.*, 1998, **120**, 6024.
- M. E. Davis, *Nature*, 2002, **417**, 813.
- F. Schüth and W. Schmidt, *Adv. Mater.*, 2002, **14**, 629.
- M. Sasaki, M. Osada, N. Higashimoto, T. Yamamoto, A. Fukuoka and M. Ichikawa, *J. Mol. Catal. A: Chem.*, 1999, **141**, 223.
- H. J. Shin, R. Ryoo, Z. Liu and O. Terasaki, *J. Am. Chem. Soc.*, 2001, **123**, 1246.
- C. M. Yang, P. H. Liu, Y. F. Ho, C. Y. Chiu and K. J. Chao, *Chem. Mater.*, 2003, **15**, 275.
- C. Garcia, Y. Zhang, F. DiSalvo and U. Wiesner, *Angew. Chem., Int. Ed. Engl.*, 2003, **42**, 1526.
- S. Inagaki, S. Guan, Y. Fukushima, T. Ohsuna and O. Terasaki, *J. Am. Chem. Soc.*, 1999, **121**, 9611.
- B. J. Melde, B. T. Holland, C. F. Blanford and A. Stein, *Chem. Mater.*, 1999, **11**, 3302.
- T. Asefa, M. J. MacLachlan, N. Coombs and G. A. Ozin, *Nature*, 1999, **402**, 867.
- S. Inagaki, S. Guan, T. Ohsuna and O. Terasaki, *Nature*, 2002, **416**, 304.
- M. J. MacLachlan, T. Asefa and G. A. Ozin, *Chem.-Eur. J.*, 2000, **6**, 2507.
- A. Stein, B. J. Melde and R. C. Schroden, *Adv. Mater.*, 2000, **12**, 1403 and references therein.
- A. P. Wight and M. E. Davis, *Chem. Rev.*, 2002, **102**, 3589.
- C. M. Yang, B. Zibrowius and F. Schüth, *Chem. Commun.*, 2003, 1772.
- Y. Q. Wang, B. Zibrowius, C. M. Yang, B. Spliethoff and F. Schüth, *Chem. Commun.*, 2004, 46.
- Y. Q. Wang, C. M. Yang, B. Zibrowius, B. Spliethoff, M. Lindén and F. Schüth, *Chem. Mater.*, 2003, **15**, 5029.
- T. E. Creighton, *Proteins: Structures and Molecular Properties*, W. H. Freeman & Co., New York, 2nd edn., 1993.

- 26 A. Galarneau, H. Cambon, F. Di Renzo, R. Ryoo, M. Choi and F. Fajula, *New J. Chem.*, 2003, **27**, 73.
- 27 M. Kruk, M. Jaroniec, C. H. Ko and R. Ryoo, *Chem. Mater.*, 2000, **12**, 1961.
- 28 F. Kleitz, W. Schmidt and F. Schüth, *Microporous Mesoporous Mater.*, 2003, **65**, 1.
- 29 F. Kleitz, S. H. Choi and R. Ryoo, *Chem. Commun.*, 2003, 2136.
- 30 X. Liu, B. Tian, C. Yu, F. Gao, S. Xie, B. Tu, R. Che, L. M. Peng and D. Y. Zhao, *Angew. Chem., Int. Ed. Engl.*, 2002, **41**, 3876.
- 31 C. J. Brinker and G. W. Scherer, *Sol-Gel Science: The Physics and Chemistry of Sol-Gel Processing*, Academic Press, San Diego, 1990.
- 32 C. M. Yang, B. Zibrowius, W. Schmidt and F. Schüth, *Chem. Mater.*, 2003, **15**, 3739.